

9-1-2013

# All-Optical Photoacoustic Detection of Absorbers in Tissue Phantoms

Jami Johnson  
*Boise State University*

Michelle Sabick  
*Boise State University*

Kasper VanWijk  
*Boise State University*

# All-Optical Photoacoustic Detection of Absorbers in Tissue Phantoms

Jami Johnson

Michelle Sabick

Department of Mechanical and Biomedical Engineering,  
Boise State University

Kasper VanWijk

Department of Geosciences,  
Boise State University

## 1 Background

Visualizing and characterizing vascular structures is important for many areas of health care, from accessing difficult veins and arteries for laboratory testing, to diagnosis and treatment of cardiovascular disease. Photoacoustic (PA) imaging, one of the fastest growing fields of biomedical imaging, is well suited for this task. PA imaging is based on the photoacoustic effect, which starts with a pulsed laser source incident on biological tissue. If the wavelength of the source matches an absorption wavelength of a chromophore within the tissue, a portion of the pulse energy is absorbed by the chromophore and converted into heat. A subsequent increase in temperature, followed by an increase in pressure occurs. Acoustic waves are emitted when this pressure relaxes, which can be detected at the surface of the tissue. PA imaging is considered absorption based, therefore spectroscopic information can be extracted. Yet, unlike purely optical imaging techniques, multiple centimeters of depth can be imaged. Vascular structures, in particular, can be viewed with high contrast using PA imaging, because the absorption coefficient of blood is up to six orders of magnitude higher than surrounding tissues [1]. Additional chromophores, such as lipids in atherosclerotic plaque, are beginning to be imaged using PA techniques in vitro [2].

Contacting piezoelectric transducers are often used for detecting acoustic waves in PA imaging. In many clinical situations, however, these transducers are unfavorable due to environmental constraints, or frequency response and spatial resolution needs [3]. The ability to image without contacting the patient, and without the need for personnel to manually control a transducer, creates the opportunity for this technique to be useful in both clinical and surgical procedures. A non-contact system has the potential to be used by practitioners who require access to the vascular system such as surgeons, nurses, and phlebotomists. An additional application of this device is as an aid for surgical procedures, such as catheter interventions. Interferometry is beginning to be explored as a method of non-contact PA imaging [4].

In this study, an experiment toward non-contact photoacoustic imaging was accomplished. A broadband interferometer was used, which measured particle velocity remotely. Absorbing structures in tissue mimicking phantoms were detected at various depths with the use of an all-optical, computer-controlled photoacoustic system.

## 2 Methods

A solid tissue phantom was created, composed of deionized water, 1% Intralipid®, and 1% agar, to mimic the light-scattering and acoustic properties of human tissue. The diameter of the phantom was 8.3 cm, and the length was 4.0 cm. Three thin-walled

polyester tubes were placed in the phantom, separated by about 2 cm along the diameter of the phantom. The tubes were placed 13 mm, 20 mm, and 34 mm below the surface of the phantom (relative to the source-side). Polycarbonate end-plates were used to hold the phantom in place, with a hole in one side for the source to pass, and a horizontal pocket in the other for the detection laser to pass. Reflective tape was placed across the pocket for improved signal detection. The experimental set-up is represented in Fig. 1.

For each tube, B-scan images were recorded. An unfocused, 1064 nm Nd:YAG laser was used as the excitation source, with a 15 ns pulse width and repetition rate of 11 Hz. The source beam was aligned with the tube, and did not move during the course of the scan. Detection of the acoustic waves was accomplished with a broadband, scanning interferometer (Polytec, PSV-400). Before each scan, an infrared dye that absorbs 1064 nm was drawn into the tube of interest. The detection beam was scanned 2.079 cm across the diameter of the phantom, with the tube in the middle of the scan. A-scan measurements (64 averages) were recorded at each 335.4  $\mu\text{m}$  increment, which combined to form B-scan images.

## 3 Results

A-scan measurements from the center of each scan, with the tube, source, and detector aligned, are shown in Fig. 2. Water absorbs 1064 nm light, therefore a wave is generated at the surface

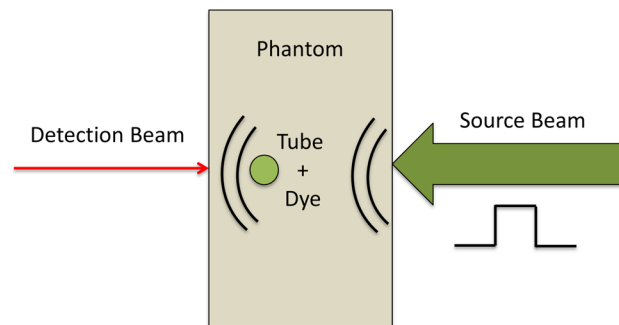


Fig. 1 Experimental set-up, with thin-walled tube and dye shown in tissue phantom. The pulsed source beam is incident on the phantom surface. Photoacoustic waves are generated at the surface and in the tube, which are detected with an interferometer on the opposite surface.

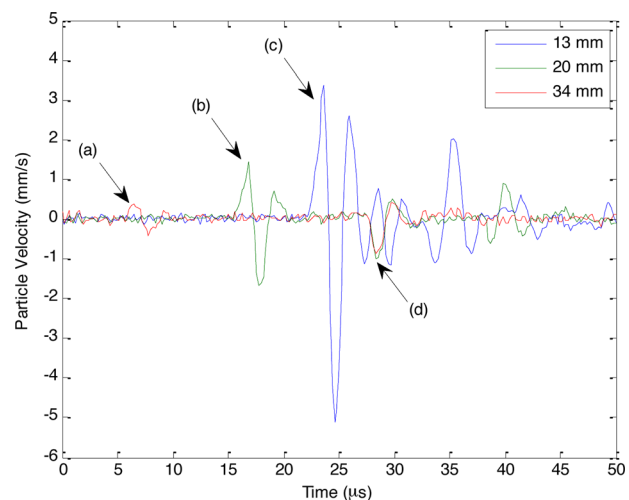
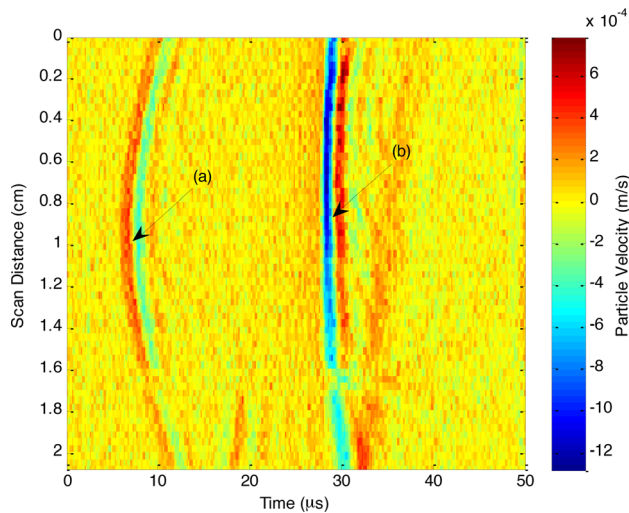


Fig. 2 A-scan measurements from middle of scan, with PA waves generated by infrared dye in tubes (a) 34 mm, (b) 20 mm, and (c) 13 mm below the surface and (d) ultrasound wave generated at the surface of the phantom (source-side).

Manuscript received March 15, 2013; final manuscript received April 29, 2013; published online July 3, 2013. Assoc. Editor: Arthur G. Erdman.

**Table 1 Measured time of arrival of waves generated at the surface of the tissue phantom, and in the tubes at various depths.**

Distance below source-surface	Measured time of arrival
0 mm (at surface)	27.2 $\mu\text{s}$
13 mm	21.3 $\mu\text{s}$
20 mm	15.0 $\mu\text{s}$
34 mm	4.3 $\mu\text{s}$



**Fig. 3 B-scan of phantom with tube and dye 34 mm below the source-surface. The wave generated (a) 34 mm below the surface and (b) at the phantom surface are indicated by arrows. The time of arrival of the waves generated at both the surface and tube increases hyperbolically as the detection beam scans away from the source and tube.**

of the phantom, in addition to the wave generated in the dye by the photoacoustic effect. Table 1 lists the time of arrival of the waves generated at the surface and in each tube. A representative B-scan is shown in Fig. 3. The wave generated at the surface,

denoted by arrow (b), propagates through the phantom, just like an ultrasound wave generated by a transducer in traditional ultrasound imaging. As a result, both an ultrasound and PA image can be obtained from the same set of data.

#### 4 Interpretation

The results of this experiment show that absorbing structures can be located and identified using an all-optical photoacoustic imaging system. The absorbing dye was representative of chromophores in the body, such as hemoglobin or lipids. These targets were detected at multiple depths in the tissue phantom, and the depth of each was confirmed by measuring the time of arrival of the PA wave generated in the dye. In addition, the ultrasound wave generated at the surface will allow for mechanical properties of structures to be exploited by examining the path of this wave.

Additional experiments will work toward taking advantage of the full capabilities of this remote imaging modality, in which both photoacoustic and ultrasound images can be obtained. Various characteristics of targets in the body will be explored, and image reconstruction will be implemented so that the absorbing structures are collapsed to actual size.

Non-contact photoacoustic detection of absorbers in the body has the potential to significantly improve medical imaging. The all-optical, computer-controlled system described has the ability to simultaneously detect a wide range of frequencies with ultimate experimental flexibility. In addition, the ability to obtain images safely, without contacting the patient, opens up an extended range of applications for clinical and surgical procedures, as well as diagnosis.

#### References

- [1] Guo, Z., Hu, S., and Wang, L. H. V., 2010, "Calibration-Free Absolute Quantification of Optical Absorption Coefficients Using Acoustic Spectra in 3D Photoacoustic Microscopy of Biological Tissue," *Opt. Lett.*, **35**(12), pp. 2067–2069.
- [2] Allen, T. J., Hall, A., Dhillon, A. P., Owen, J. S., and Beard, P. C., 2011, "Spectroscopic Photoacoustic Imaging of Lipid-Rich Plaques in the Human Aorta in the 740 to 1400 nm Wavelength Range," *J. Biomed. Opt.*, **17**(6), p. 061209.
- [3] Balogun, O., and Murray, T. W., 2011, "Frequency Domain Photoacoustics Using Intensity-Modulated Laser Sources," *Nondestructive Testing and Evaluation*, **26**(3–4), pp. 335–351.
- [4] Rousseau, G., Gauthier, B., Blouin, A., Monchalain, J. P., "Non-Contact Biomedical Photoacoustic and Ultrasound Imaging," *J. Biomed. Opt.*, **17**(6), p. 061217.